# SUPPORTING INFORMATION

## Ionic Control over Ferroelectricity in 2D Layered van der Waals Capacitors

Sabine M. Neumayer[1], Mengwei Si[2], Junkang Li[2], Pai-Ying Liao[2], Lei Tao[3,4], Andrew O'Hara[3], Sokrates T. Pantelides[3,5], Peide D. Ye[2], Petro Maksymovych[1], Nina Balke[1,6*]

[1] Center for Nanophase Materials Sciences, Oak Ridge National Laboratory, Oak Ridge, 37831 TN, USA
E-mail: balken@ornl.gov

[2] Birck Nanotechnology Center and School of Electrical and Computer Engineering, Purdue University, West Lafayette, Indiana 47907, USA

[3] Department of Physics and Astronomy, Vanderbilt University, Nashville, Tennessee 37235, USA

[4] University of Chinese Academy of Sciences & Institute of Physics, Chinese Academy of Sciences, Beijing 100190, China

[5] Department of Electrical and Computer Engineering, Vanderbilt University, Nashville, Tennessee 37235, USA

[6] Department of Materials Science and Engineering, North Carolina State University, Raleigh NC 27695-7907, USA

*Corresponding author:
Nina Balke, ninabalke@ncsu.edu

## I. Current at the beginning and end of DC voltage pulses

We investigate the current at the beginning (Figure S1(a)) and end (Figure S1(b)) of the DC voltage pulse. When the DC voltage pulse is turned on, ferroelectric switching events are visible as current peaks (Figure S1(a)) and indicate the poling process of the capacitor. The corresponding total switched polarization is shown in Figure S1(c). It is approximately between -8 and -10 µC/cm$^2$, which is about twice the reported remnant polarization and therefore indicates switching of the polarization vector from -c to +c orientation. This behavior is expected since the measurements are performed sequentially and the last applied voltage during the fast voltage sweeps is of positive polarity (Figure 2(a)). In addition, currents appearing at the end of the pulses are also observed and are strongly dependent on the DC pulse duration (Figure S1(b)). After pulses of 4, 10 and 20 ms duration, that do not activate ionic currents, *I* decreases to zero when the voltage pulse is turned off. If ionic currents are activated, at the end of the 100, 200 and 400 ms pulses, a positive current peak appears, corresponding to a total switched polarization of 0.4, 2, and 5.7 µC/cm$^2$, respectively (Figure 2(c)). For 500 ms and 600 ms, negative current peaks indicate a change in polarization of -3.5 and -2.7 µC/cm$^2$. For 800 and 900 ms pulses, no clear current peaks are observed and large currents are still measurable after the voltage has been turned off, which we interpret as relaxation of the ionic current. We hypothesize that the switching currents at the end of the DC voltage pulse can be interpreted as the formation of domains. Large ionic currents introduce disorder but since the measurements are below the Curie temperature, the ordered ferroelectric state re-forms after the voltage pulse. At this point, it is unclear how this process unfolds, but the experimental data suggest it involves first the formation of positively oriented domains which transition into negatively oriented domains as the DC voltage pulses become longer and more disorder is introduced.

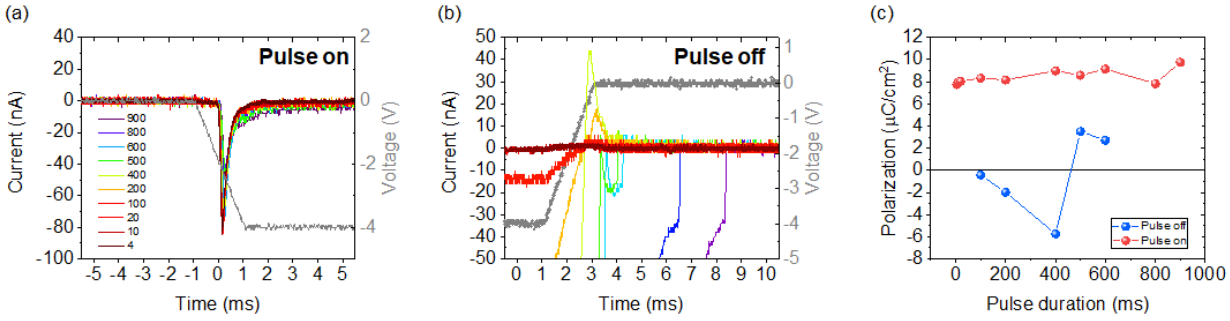


**Figure S1.** (a) Current measured at the start of the square pulses. (b) Current measured at the end of the pulses. Time scales shifted to show the end of the pulse at the same time. (c) Polarization change during pulse on and off as a function of pulse duration.

## II. Symmetric behavior at positive DC pulses

While negative DC pulses lead to negative currents in subsequent triangular pulses, the situation is symmetric for positive set pulses. In this case, positive DC pulses lead to positive ionic currents during the DC pulse and the positive part of the triangular voltage sweep (Figure S2)

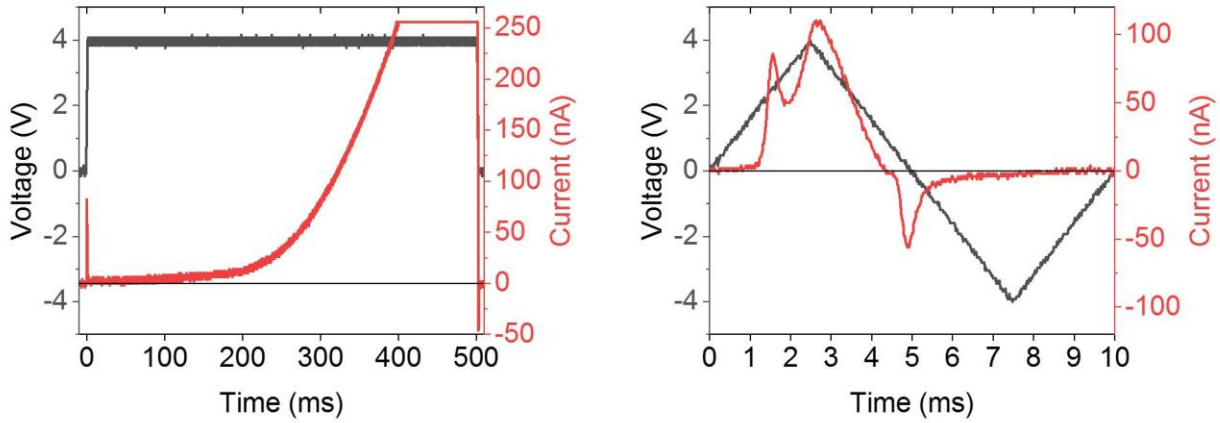


**Figure S2.** Current during positive set pulse of 500 ms (left) and subsequent triangular voltage sweep (right).

## III. Separation of ionic and polarization switching current

In order to separate the ionic and ferroelectric switching current, the total current is plotted as function of time and is fitted using 4 Gaussian distributions. Where the current is outside the current-measurement range, the fit provides an extrapolation of the ionic current, which is shown in the main text.

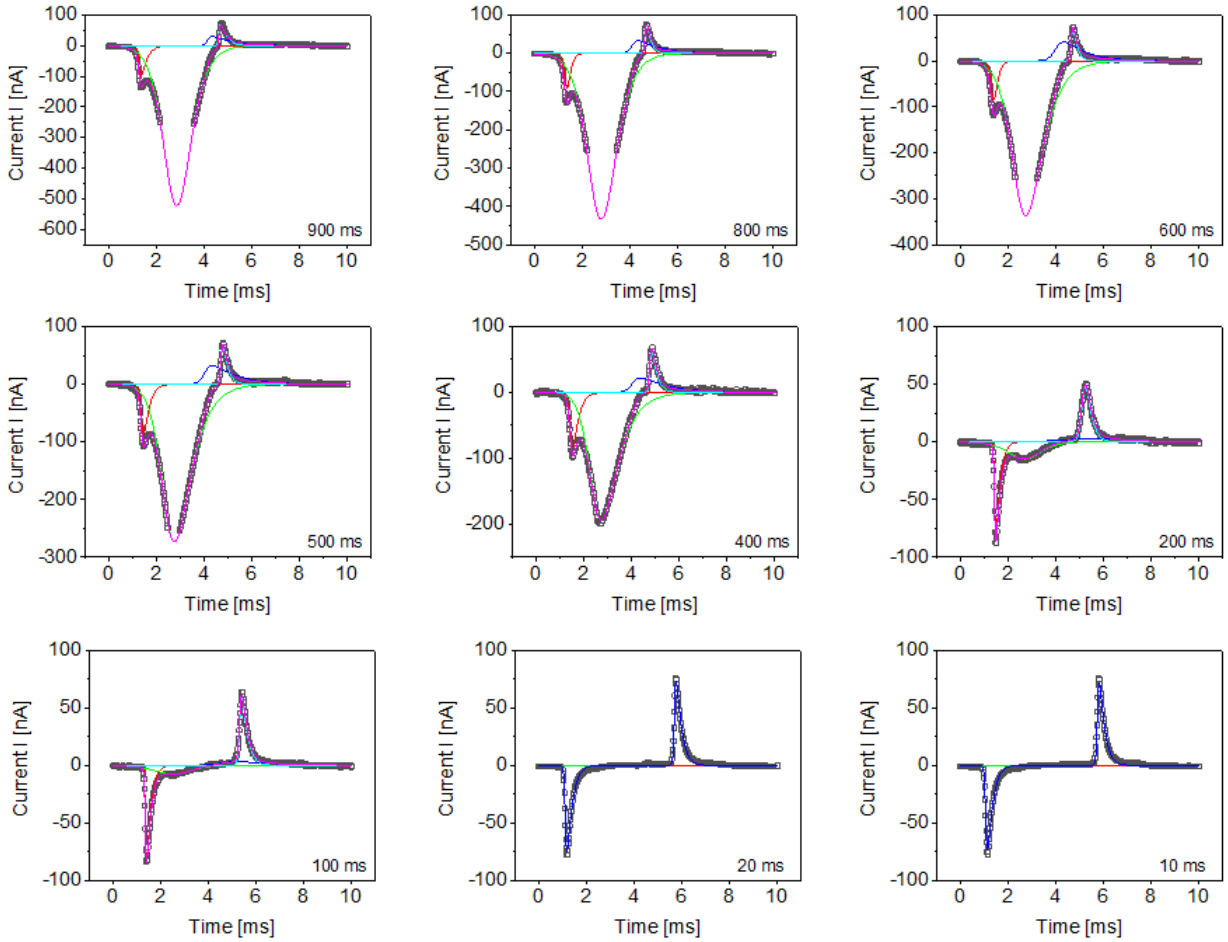


**Figure S3.** Four-peak fitting of currents measured during the triangular voltage sweep to differentiate between ionic currents and the two polarization switching peaks at negative and positive voltages. The purple (100 ms to 900 ms) and blue (10 ms and 20 ms) curves show the overall fit. The additional peak in blue (400 ms to 900 ms) is an ionic contribution similar to the current peaks observed when longer DC voltage pulses are turned off.

### III. Ionic current, ionic charge, and corresponding CIPS layer number

Here we explain how to calculate the ionic charge and the corresponding number of CIPS layers under the electrode that are necessary to provide the amount of charge required for the measured ionic currents. These calculations do not refer to the total number of CIPS layers across the entire sample thickness. The integral of the fitted ionic current contribution is used to determine the ionic charge $Q_i$. We assume that each Cu can take one electron according to $Cu^+ + e^- \rightarrow Cu$ accounting for a charge of $1.6022 \cdot 10^{-19}$ As. The amount of charge per CIPS layer is calculated by considering the number of unit cells in one layer under the electrode area ($20 \times 20$ µm$^2$) using cell parameters a=6.11542 Å and b=10.58783 Å with two Cu ions being

present in each layer per these unit cell dimensions. We obtain a charge per CIPS layer of $Q_{layer} \approx 0.198$ nC. The number of layers needed to provide the ionic charge is then the ionic charge divided by the layer charge.

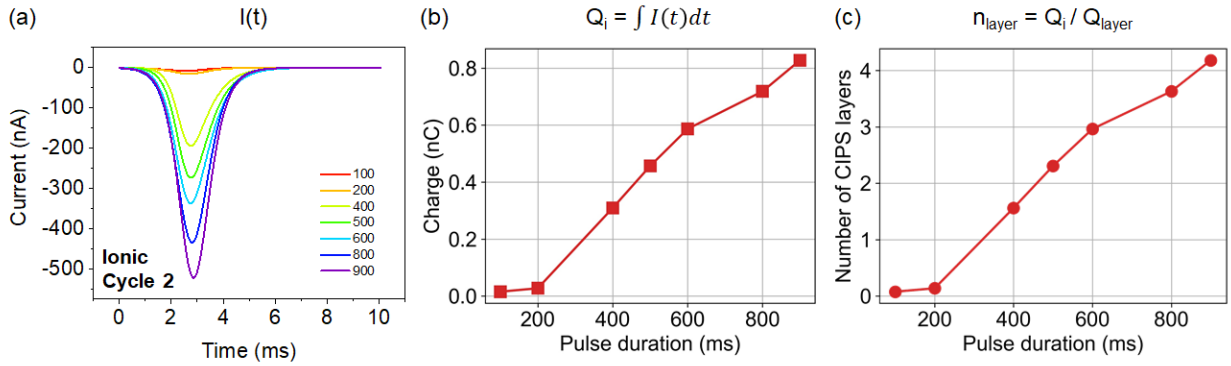


**Figure S4.** (a) Ionic current, (b) ionic charge $Q_i$ and (c) the number of CIPS layers needed to provide the ionic charge as function of DC voltage pulse duration.

## IV. Polarization hysteresis area analysis

The area of the P(V) loops in Figure 2(c) corresponds to an energy. Figure S5 provides the loop area in units of energy as function of DC voltage pulse duration.

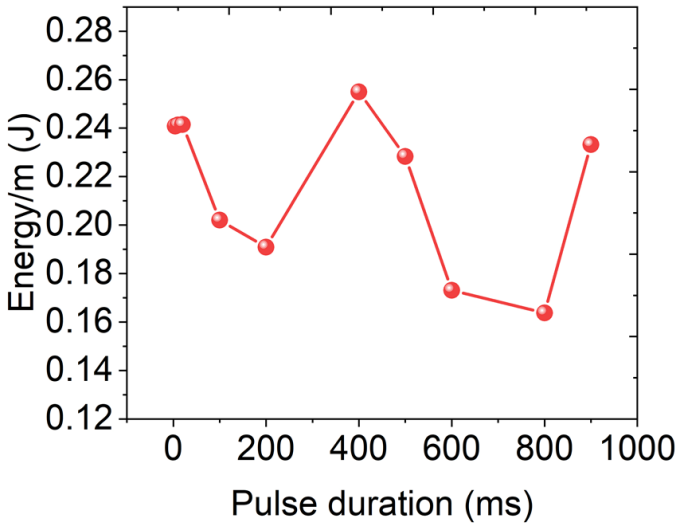


**Figure S5.** Work as a function of DC voltage pulse duration calculated from the area of the polarization vs voltage loops in Figure 2(c).

## V. Ionically induced polarization changes as function of cycle number

To investigate the persistence of changes in ferroelectric and ionic behavior initiated by the DC voltage pulses, we probed currents during 10 triangular cycles that follow square pulses of 20 ms, 500 ms and 1000 ms at -6 V (Figure S6(a)) on a virgin capacitor sample. The CIPS layer in this sample of ~420 nm was thicker than the previous sample shown in Figure 1, which is why a higher voltage of 6 V was selected. The 20 ms pulse does not result in measurable ionic currents and only one switching peak is measured, whereas 500 ms and 1000 ms pulses resultin ionic currents up to -40 nA and -160 nA, respectively (Figure 7). After the 20 ms pulse, typical ferroelectric switching current peaks are measured during all of the 10 subsequent triangular cycles (Figure S6(b)). Ionic currents appear during triangular cycles after the 500 ms (Figure S6(c) and (d)). The first 5 cycles show ionic currents at negative $V$ in addition to the ferroelectric switching currents. The ionic-current contribution decreases as a function of cycle number and vanishes at cycle #6. At a longer DC pulse of 1000 ms, which activates a higher ionic current, the ionic behavior impacts all switching cycles, albeit to a lesser degree at later cycles (Figure S6(d)). Therefore, the maximum ionic current during triangular $V$ sweeps is a function of both DC-voltage-pulse duration and cycle # (Figure S6(e)). The longer the pulse, the higher the ionic current, which decreases exponentially with every cycle. If Cu ion accumulation under one electrode can be ascribed to the fast ionic current component, the decrease of ionic current as function of cycle number can be explained by spontaneous Cu redistribution based on the induced concentration gradient, which would increase the distance between Cu ions and the electrode and, therefore, reduce the fast ionic current component. The DC voltage pulse strongly affects the positive coercive voltage $V_c^+$, which decreases with increasing DC voltage pulse duration but is relatively unchanged for subsequent cycle numbers (Figure S6(f)). $V_c^-$ on the other hand, is approximately constant around 4 V. This observation is consistent with the behavior shown in Figure 2(e), where $V_c^+$ changes more significantly with increasing pulse duration than $V_c^-$. Moreover, we can conclude that ionic behavior activated by long DC pulses has a lasting impact on $V_c^+$, i.e., on polarization switching, even in the absence of ionic currents at later cycles. It should be mentioned that the results in Figure S6 and Figure 2 are not directly comparable since they were conducted on different capacitors with different coercive voltages and different values of ionic current.

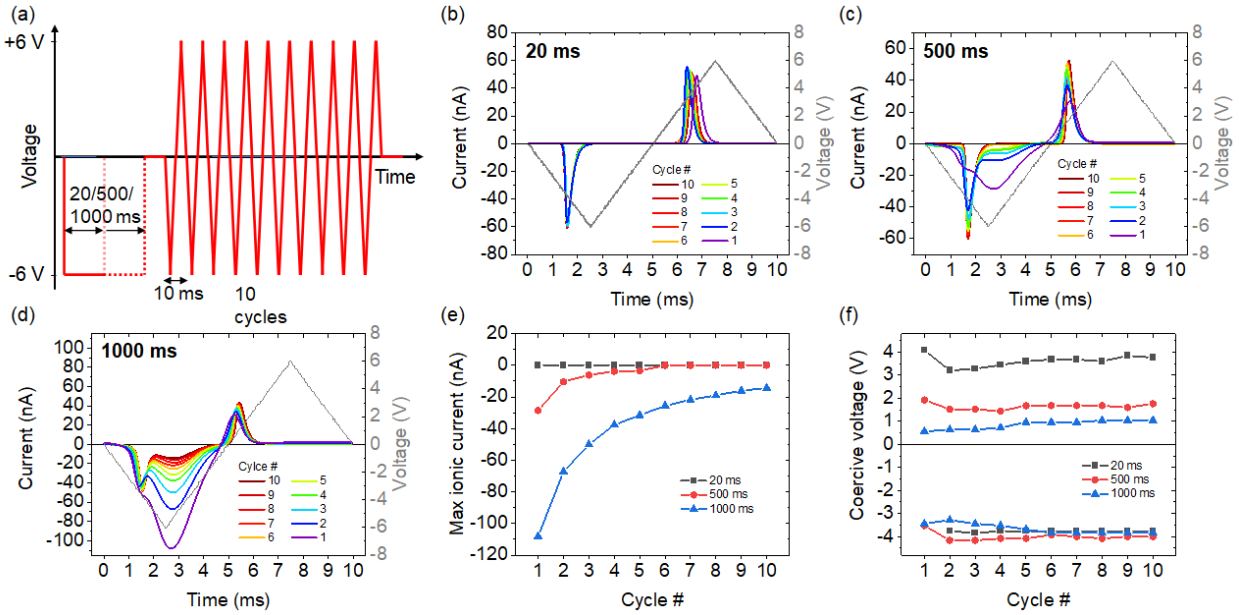


**Figure S6.** (a) Scheme of waveform consisting of a -6V square pulse of either 20, 500 or 1000 ms followed by 10 triangular cycles of 10 ms duration. Current during the triangular cycles after (b) 20 ms, (c) 500 ms and (d) 1000 ms square pulses. (e) Maximum ionic current during triangular cycling after 20, 50, and 1000 ms pulses. (f) Positive and negative coercive voltages for all 10 cycles after 20, 50, and 1000 ms pulses.

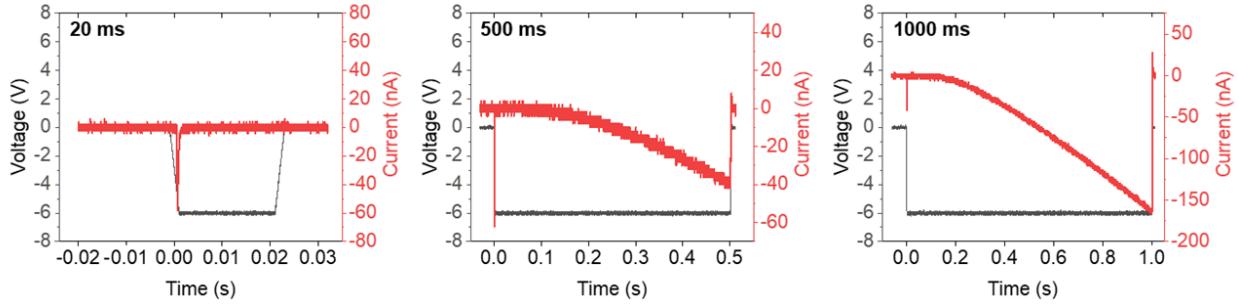


**Figure S7.** Current during square DC voltage pulses of 20 ms, 500 ms and 1000 ms duration.

### VI. Density of states calculations

In order to understand how the migration of copper affects the electronic structure of the system, we perform a layer-by-layer analysis of the density of states for each polarization state of the Ni/*m* $InP_2S_6$/*n* $CuInP_2S_6$/Cu/Ni system, shown in Figure S8. The outermost layers (L1 and L6) are always metallic regardless of Cu content due to contact doping with the Ni contact. Initially (Figure S8(a)), the middle four layers (L2, L3, L4 and L5) are insulating regardless of polarization state. However, after one or more layers of Cu have moved across the gap, there are now layers of $InP_2S_6$. $InP_2S_6$ can be considered either as Cu-

deficient $CuInP_2S_6$ or In-deficient $In_{4/3}P_2S_6$. Being heavily cation deficient in either perspective indicates that the $InP_2S_6$ layers are likely to be metallic. We confirm this via the density of states for $InP_2S_6$ in Figure S9 and show a comparison to stoichiometric $In4_{/3}P_2S_6$ which is not metallic.

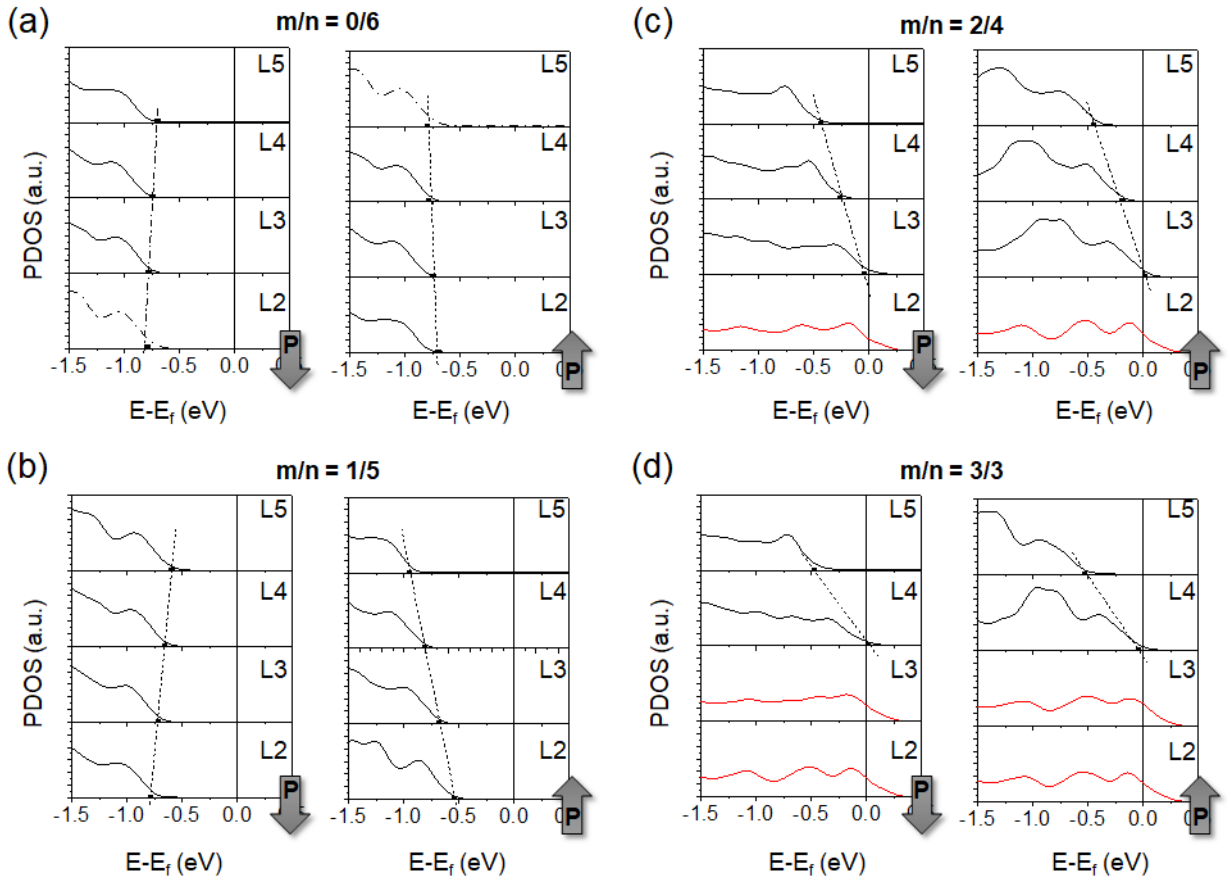


**Figure S8.** Layer projected density of states projected for the n-$CuInP_2S_6$/m-$InP_2S_6$ system with (a) m/n=0/6, (b) m/n=1/5, (c) m/n=2/4, (d) m/n=3/3 for downward and upward oriented polarization, respectively. See Figure 3 in the main text for atomistic structures. Electrically insulating layers are drawn in black, conductive layers are drawn as red lines. Layers L1 and L6 are omitted as they are fully metallic due to contact doping in all cases.

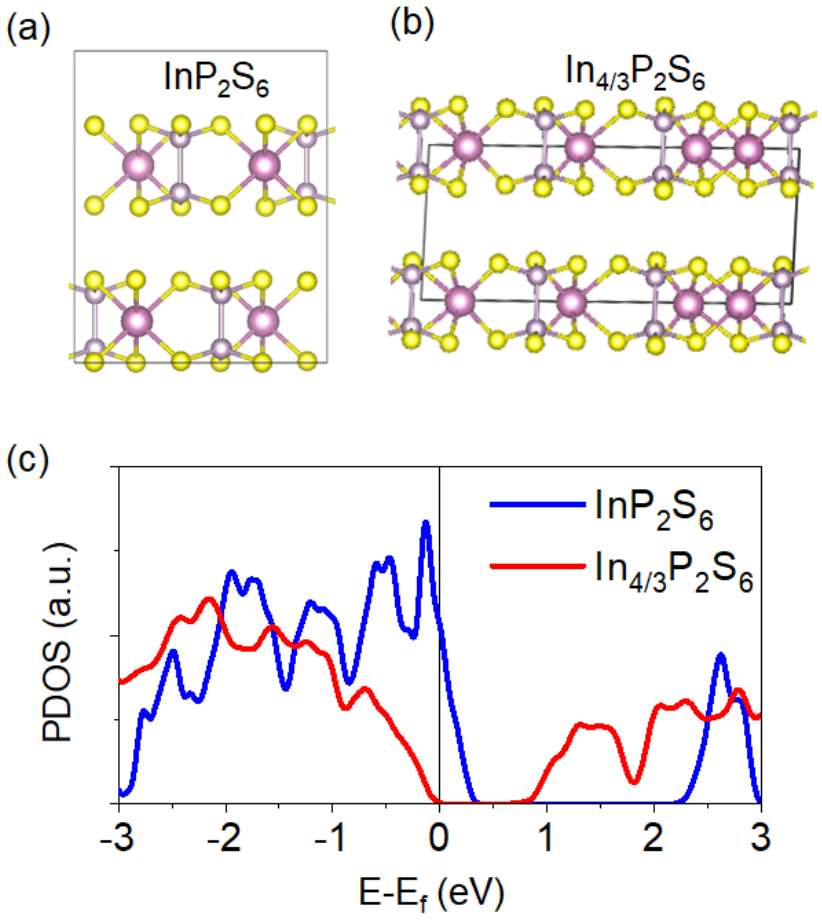


**Figure S9.** Structures of (a) $InP_2S_6$, that corresponds to the structure of $CuInP_2S_6$ in which all Cu atoms are missing, and (b) $In_{4/3}P_2S_6$. (c) Density of states of $InP_2S_6$ and $In_{4/3}P_2S_6$.

**VII. Determination of internal electric field and polarization from DFT**

Both the ferroelectric polarization and the movement of Cu atoms create internal electric fields of varying strength which manifest in a gradient of the valence-band edge position of each layer (*i.e.*, band bending). In the m = 0 cases, the significant distortion in layer 1 (layer 6) for the down (up) case causes an additional distortion of some Cu atoms in the adjacent layer 2 (layer 5) which causes a shift of the valence band edge unrelated to the band bending effect from the electric field. Therefore, these layers were not used in calculating the fields for the m = 0 case. The black dashed line in Figure S8 is placed connecting the valence-band edges in the insulating layers. The slope of this curve is indicative of the electric field value. In Figure S10(a), we show all valence band edges for each of the cases. The sign of the slope (positive or negative)

refers to the direction of internal electric field (up or down). These are the fields that are then plotted in Figure 4(b) in the main text and indicate the build-up of an internal field caused by the ionic migration of Cu atoms.

The value of the spontaneous polarization for each slab is shown in Figure S10(b). The polarization is estimated by averaging the Cu displacement relative to the mid-layer centrosymmetric plane for each insulating layer of a given slab and comparing it to the nominal bulk values for a given displacement. The black dash line is the polarization as a function of Cu displacement in a periodic CIPS.

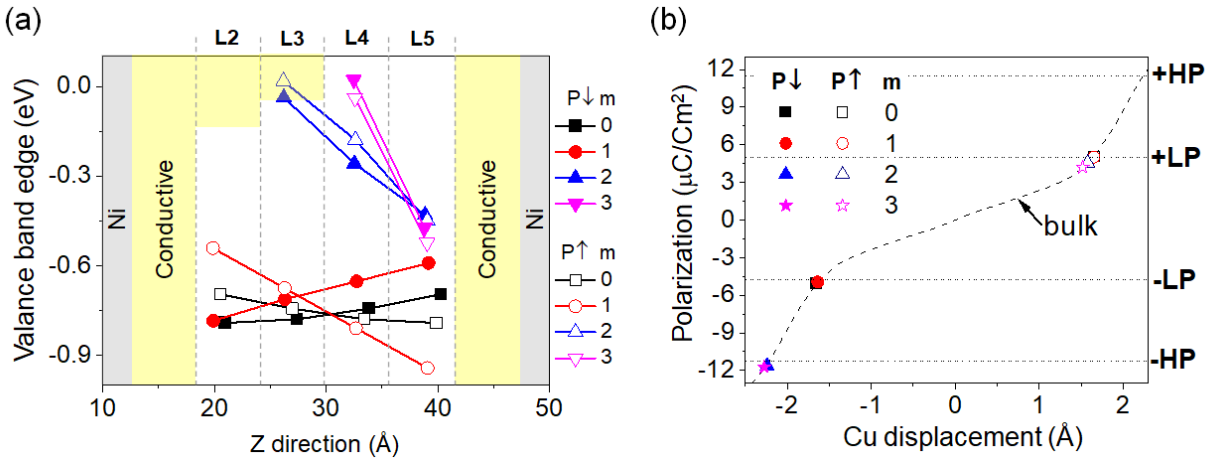


**Figure S10.** (a) Valence-band edge of each insulating layer in each of the considered n/m configurations, according to PDOS in Figure S8. (b) Estimated polarization in each state according to the average Cu displacement. The black dash line is the polarization as a function of Cu displacement in a periodic CIPS. The horizontal blue dashed lines indicate the polarization values for the bulk polarization states.